Published in final edited form as:
Polyhedron. 2013 July 13; 58: 179–189. doi:10.1016/j.poly.2013.01.043.

Sulfide Oxidation by O_2: Synthesis, Structure and Reactivity of Novel Sulfide-Incorporated Fe(II) Bis(imino)pyridine Complexes

Leland R. Widger, **Maxime A. Siegler**, and **David P. Goldberg**
Department of Chemistry, The Johns Hopkins University, 3400 N. Charles Street, Baltimore, MD 21218

Abstract

The unsymmetrical iron(II) bis(imino)pyridine complexes $[Fe^{II}(LN_3SMe)(H_2O)_3](OTf)_2$ (**1**), and $[Fe^{II}(LN_3SMe)Cl_2]$ (**2**) were synthesized and their reactivity with O2 was examined. Complexes **1** and **2** were characterized by single crystal X-ray crystallography, LDI-MS, ^{1}H-NMR and elemental analysis. The LN_3SMe ligand was designed to incorporate a single sulfide donor and relies on the bis(imino)pyridine scaffold. This scaffold was selected for its ease of synthesis and its well-precedented ability to stabilize Fe(II) ions. Complexes **1** and **2** ware prepared via a metal-assisted template reaction from the unsymmetrical pyridyl ketone precursor 2-(O=CMe)-6-(2,6-(^{i}Pr$_2$-C$_6$H$_3$N=CMe)-C$_5$H$_3$N. Reaction of **1** with O_2 was shown to afford the S-oxygenated sulfoxide complex $[Fe(LN_3S(O)Me)(OTf)]^{2+}$(**3**), whereas compound **2**, under the same reaction conditions, afforded the corresponding sulfone complex $[Fe(LN_3S(O_2)Me)Cl]^{2+}$ (**4**).

Keywords

bis(imino)pyridine; sulfide; iron(II); dioxygen; sulfoxide; sulfone

1. Introduction

There is broad interest in understanding the mechanisms by which metalloenzymes activate O_2 and control reactivity with substrates [1]. Many non-heme iron oxygenases that carry out these reactions typically employ a 2-His-1-carboxylate motif around the catalytically active iron center. One exception is cysteine dioxygenase (CDO), which contains a high-spin ferrous center bound by three His residues in a facial triad and one water molecule completing a pseudo-tetrahedral coordination sphere. This $(His)_3Fe^{II}$ (H_2O) center likely activates O_2 upon binding of the cysteine substrate, and is responsible for catalyzing the oxidation of cysteine to cysteine sulfinic acid (Fig. 1). Mechanistic information for many non-heme iron dioxygenases is available [2-7], but little is known about the mechanism of CDO. There is debate in the literature about the nature of the possible O_2 derived intermediate(s) in the catalytic cycle of CDO [8-18]. As the first step in mammalian cysteine

Correspondence to: David P. Goldberg.

Appendix A. Supplementary data: ^{1}H-NMR, UV-Vis, EPR and IR spectra, UV-Vis titration data, calibration curve and standard spectra for $[Fe(phen)_3]^{2+}$ and $[Fe(phen)_3]^{3+}$. CCDC 897768 and 897769 contain the supplementary crystallographic data for **1** and **2**. These data can be obtained at http://www.ccdc.cam.ac.uk/conts.retrieving.html, or from the Cambridge Crystallographic Data Centre, 12 Union Road, Cambridge CB2 1EZ; fax (+44) 1223-336-003; or e-mail: deposit@ccdc.cam.ac.uk.

catabolism, CDO activity is critical for proper cellular function. Loss of this activity has been implicated in many disease states including cystinosis [19, 20], Hallervoden-Spatz syndrome [21], Alzheimer's and Parkinson's disease [22, 23].

In addition to the biological relevance of sulfur-oxidation, sulfoxides are valued synthetic intermediates to organic chemists [24, 25] and are important in many pharmaceutically active compounds (Fig. 2a) [26-28]. Sulfur oxidation is a well-known and widely used synthetic strategy for a variety of applications in organic chemistry [29], but the use of stoichiometric amounts of harsh or toxic oxidizing agents (Fig. 2b) and the difficulty of stopping oxidation at the sulfoxide [30, 31] presents challenges that have attracted the interest of inorganic chemists. Furthermore, sulfoxidation catalysts have recently attracted a great deal of attention for use in desulfurization of fossil fuels with O2 and other applications to reduce toxicity (Fig. 2c) [28, 32, 33].

Some metal-based systems have been developed to oxidize sulfides under mild conditions. Some of these systems perform as catalysts for asymmetric sulfide oxidation, and a few can utilize dioxygen as the oxidant [34-60]. There are only a few reports of iron-based sulfoxidation catalysts, but all of these systems utilize Fe^{III} centers in lieu of Fe^{II} [41, 49, 51, 52]. Molecular O_2 is used in some of these cases as a co-oxidant with an Fe^{III} source and an additional oxidant generated in situ. For example, Wang and coworkers have reported a catalytic Fe_2O_3 system where molecular oxygen is proposed to work in concert with the Fe^{III} catalyst to generate peracid oxidants in situ from various aldehydes [44, 45]. These peracids, much like mCPBA, are ultimately responsible for sulfide oxidation. Despite the efficiency of the Wang Fe_2O_3/O_2/aldehyde system, only modest yields are observed for sulfone products. In addition, peracids are not selective for sulfides, and are well known to be efficient reagents for olefin epoxidation, Baeyer-Villiger oxidation of ketones, and oxidation of secondary alcohols, even in the absence of a metal catalyst [43]. This limited functional group tolerance severely restricts the scope under which this methodology could be used in a synthetic scenario. In other systems reported by Rossi et al., [49, 51, 61, 62] aerobic oxidation is carried out by catalytic amounts of NO_2 (which is in equilibrium with N_2O_4), generated by an $FeBr_3$ catalyst from HNO_3. In these reports, once NO_2/N_2O_4 is generated there is an aerobic catalytic cycle of NO_2 species which gives NO and the S-oxygenated product. NO then reacts with O_2 to regenerate NO_2 and turnover the system (Fig. 3). Recent mechanistic studies have actually shown that these types of systems, originally reported with $FeBr_3$ to initiate the catalytic reaction, can in fact proceed in the absence of a metal-based catalyst [61, 63]. Catalytic systems based solely on these types of gaseous equilibria are sensitive to a variety of environmental conditions, and are likely to be deactivated in many industrial circumstances [52].

Recent work in our lab has focused on the development of iron(II) complexes with mixed N/S donor sets to serve as structural and functional models for a variety of non-heme metalloenzymes, including non-heme iron oxygenases which utilize O_2 for substrate oxidation reactions. Previous reports from our lab have included examples where an Fe^{II} center was shown to mediate sulfur oxygenation of thiolate ligands [64-66]. In these reports, discrete thiolate-ligated Fe^{II} complexes reacted with O_2 at room temperature and atmospheric pressure to give the corresponding Fe^{II}-sulfonato or sulfinato complexes. In addition to being among the first reports of this reactivity [64-67], the assignment of an oxidation state for the product as Fe^{II} was interesting due to the similarity with the iron(II) resting state in CDO. We were interested in synthesizing a modified $(LN_3SMe)X_2$ system which incorporated sulfides in place of the thiolate **V**donors to determine the effect on S-oxygenation reactivity. Herein we report the synthesis, characterization, and O_2 reactivity of two novel methyl-sulfide iron(II) complexes. The unsymmetrical bis(imino)pyridine complexes $[(Fe^{II}(LN_3SMe)(H_2O)_3](OTf)_2$ (**1**) (Fig. 4) and $[Fe^{II}(LN_3SMe)Cl_2]$ (**2**) (Fig. 5),

were synthesized by metal-assisted template reactions. Complexes **1** and **2** were characterized by single crystal X-ray crystallography, LD-MS, ^{1}H-NMR, and elemental analysis. Complex **1** reacts with O_2 at modestly elevated temperature to afford the sulfoxide complex $[(Fe(LN_3SOMe)(OTf)]^{2+}$ (**3**), while **2**, under the same conditions, yields the sulfone complex $[Fe(LN_3SO_2Me)Cl]^{2+}$ (**4**).

2. Results and Discussion

2.1. Synthesis of LN_3SMe Complexes

The bis(imino)pyridine (BIP) ligand scaffold has been widely used due to its ease of synthesis, and facile steric and electronic modification to give a range of ligand variants. In fact, from commercially available 2,6-diacetylpyridine and 2 equiv of a primary amine, it is possible to synthesize a large array of symmetrical BIP ligands in one pot in a matter of hours. The challenge lies in the synthesis of unsymmetrical derivatives, of interest to us so as to be able to incorporate sulfur-containing functional groups around the metal center. For our purposes regarding iron-oxygen chemistry, a key requirement for a ligand system is to be able to include significant steric protection around the metal center to help prevent the formation of polymeric Fe complexes. We were therefore fortunate to come across the unsymmetrical precursor 2-(O=CMe)-6-(2,6-(^{i}Pr$_2$-C$_6$H$_3$N=CMe)-C $_5$H$_3$N, reported by Bianchini and coworkers [68], which is easily prepared by mixing 2,6-diacetylpyridine and 2,6-diisopropylaniline in MeOH with catalytic formic Vacid. The product is insoluble in MeOH and precipitates out of solution before it can react further. This precursor includes pre-organized steric shielding via the 2,6-diisopropylphenyl substituent, and it provides a convenient way for installing a single sulfur-containing group through the available ketone (see Schemes 1 and 2).

We have previously reported the difficulty in direct condensation, or even reductive amination, of the second amine onto this unsymmetrical precursor [69]. The difficulty we encountered while attempting to synthesize these ligands resulted from the reversibility of the Schiff-base reactions. Extended exposure of the unsymmetrical precursor to Schiff base reaction conditions may lead to scrambling of the imine groups, giving intractable mixtures of labile imine products [69]. However, pre-binding a metal ion to the 2-(O=CMe)-6-(2,6-(^{i}Pr2-C$_6$H$_3$N=CMe)-C$_5$H$_3$N precursor alleviates this problem, and by using this metal template method we have been successful at synthesizing several unsymmetrical, BIP-derived compounds with an array of metal ions.

A template reaction was carried out to synthesize the new iron(II)-sulfide complexes $[Fe^{II}(LN_3SMe)(H_2O)_3](OTf)_2$ (**1**), and $[Fe^{II}(LN_3SMe)Cl_2]$ (**2**). The appropriate Fe^{II} salt ($Fe(OTf)_2$ or $FeCl_2$) was suspended in EtOH with 2-(O=CMe)-6-(2,6-(^{i}Pr$_2$-C$_6$H$_3$N=CMe)-C$_5$H$_3$N and heated to 60 °C for 1 h, or until all of the solids dissolved. As the solids dissolve, the solution becomes deep purple or blue in color for the trifuloromethanesulfonate or chloride complexes, respectively. This step is followed by addition of 2-(methylthio)aniline added together with Et_3N, and the reaction mixture is allowed to stir at 80 °C for 24 h. The crude reaction mixture is then concentrated to a residue and transferred to the glovebox for crystallization. Single crystals suitable for X-ray structure determination were grown from vapor diffusion of diisopropyl ether into **V**solutions of **1** (in MeCN) and **2** (in MeOH). Crystallographic data for complexes **1** and **2** are summarized in Table 1.

2.2. X-ray crystallography

The ferrous center of **1** is bound in a distorted octahedral geometry by the three neutral N donors from the BP ligand and three water molecules (Fig. 4). Although Fe^{II}-bis(imino)pyridine complexes are usually found in five-coordinate geometries, there are a

few reported examples of octahedral complexes [65, 70]. The aryl diisopropyl group is projected orthogonal to the N_3 plane, which contains the iron ion. The three water molecules lie in a plane completing the octahedral coordination environment; the locations of all H atoms from the three water ligands were easily derived from the difference Fourier maps. The sulfide moiety is not bound to the iron center, being displaced by the water molecules from the coordination sphere. The asymmetric unit contains three trifluoromethanesulfonate anions, one triethylammonium cation, and the Fe complex, leading to the assignment of the metal center as iron(II).

The structure of **2** is shown in Fig. 5. The three neutral bis(imino)pyridine N donors and two chloride anions bind the ferrous center in a distorted square pyramidal geometry ($\tau = 0.18$). The diisopropyl groups are projected orthogonal to the N_3 plane in which the iron sits, and as in **1** the sulfide moiety is not bound to the iron center. One chloride counterion occupies the axial position while the second occupies a pseudoequatorial position completing the square pyramid. Additionally there is one uncoordinated lattice solvent methanol molecule per Fe complex in the structure of **2**.

Bond distances for complexes **1** and **2** are consistent with high-spin ferrous centers [71] and are in good agreement with similar bis(imino)pyridine compounds reported in the literature [65, 70, 72]. A comparison of bond lengths from cations **1** and **2** with closely related compounds in the literature are summarized in Table 2. The comparable symmetrical analogue of complex **1**, $[Fe^{II}(^{iPr}BIP)(H_2O)_2(NCCH_3)](OTf)_2$, reported previously by our lab [65] has an additional diisopropyl phenyl group in lieu of the aryl sulfide substitution. In addition, $[Fe^{II}(^{iPr}BIP)(H_2O)_2(NCCH_3)](OTf)_2$ has two axial water ligands and an equatorial coordinated acetonitrile molecule, while **1** has 3 coordinated water molecules. Fe-N_{imine} and Fe-N_{pyr} distances of 2.276(3), 2.280(3) and 2.075 Å are in good agreement with the observed Fe-N distances of 2.245(2), 2.234(2) and 2.102(2) Å in **1**. Fe-OH_2 distances in the symmetrical $[Fe^{II}(^{iPr}BIP)(H_2O)_2(NCCH_3)](OTf)_2$ complex are 2.075(2) and 2.161(2) Å, very close to the observed Fe-OH_2 distances in **1** of 2.086(2), 2.098(2) and 2.116(2) Å, while N_{imine} -C_{imine} distances are very much comparable. Similar results are derived from comparison of **2** with the closely related symmetrical bis(diisopropylphenyl) compound $[Fe^{II}(^{iPr}BIP)Cl_2]$, first reported by Brookhart and coworkers [72] (see Table 2). The observed bond angles in **1** and **2** are also in good agreement with their close analogues from the literature (Table 2).

In the solid-state structure of **1**, there does not appear to be any **π**-stacking interactions between the individual cations of **1**, as all of the aryl groups are significantly offset from each other. In fact, the individual cations are angled away from each other in order to accommodate an extensive H-bonding network (Fig. 6). In this network, two of the three trifluoromethanesulfonate anions (containing S2 and S4) are found to be H-bond acceptors in two O-H…O hydrogen bonds, for which the coordinated water molecules (O1, O2 and O3) are donors. One of the trifluoromethanesulfonate ions bridges the cations of **1** between O2… O5 and O4… O3 through H-bonds, where O2 and O3 are the two axially coordinated water molecules, and O4 and O5 are from the trifluoromethanesulfonate ion. The remaining trifluoromethanesulfonate anion (containing S3) is found to be an H-bond acceptor in O_{Water} –H…O and N–H…O H-bonding water interactions (the triethylammonium cation is the donor in the latter). Distances and angles for H-bonds in the solid state structure of **1** are given in Table 3. All values are consistent with good H-bonding interactions and are in good agreement with accepted values (D-A ≈ 2.6 – 2.7 Å, DHA ≥ 160°) although some variation is expected based on the nature of the individual H-bond.

2.3. NMR Spectroscopy

Compounds **1** and **2** were characterized by ^{1}H-NMR spectroscopy. Both compounds exhibit paramagnetically shifted peaks, consistent with the assignment of high-spin Fe^{II} from metal-ligand bond distances. The ^{1}H-NMR spectrum for **1** exhibits peaks that are paramagnetically shifted from 90 ppm to −42 ppm, while for **2** a wider spread of resonances are observed, from 97 ppm to −38 ppm (Figs. S1 - S2). The spectra for compounds **1** and **2** are significantly more complex relative to related, symmetrical BIP complexes that we have prepared [65], likely due to the desymmetrized nature of **1** and **2**, as well as the possibility for ligand exchange at the metal center on the NMR timescale. Although individual resonances cannot be assigned in the spectra of **1** and **2**, the spectra are consistent and reproducible for analytically pure samples.

2.4. O_2 Reactivity

General Remarks—All O_2 reactions were carried out in a sealed reaction vessel, equipped with a vacuum port that was connected above the Teflon screw-cap. Solutions of compounds **1** and **2** in CH_2Cl_2 were transferred to the flask, and then the flask was charged with O_2 by bubbling directly into the CH_2Cl_2 solution for 5 min. The vessel was then sealed and heated to 60 °C for several days. Typical reaction times varied from 24 to 96 h, depending on concentration and reaction scale.

2.4.1. S-Oxygenation Reactions—Although compound **1** is unreactive toward O_2 at ambient temperature and pressure, a new sulfoxide product is generated at modestly elevated temperature in CH_2Cl_2, as seen in Scheme 3. The reaction of **1** to **3** was followed by LDI-MS. As shown in Fig. 7, a loss of the starting material at *m/z* 648.1 ([**1** - 3 H_2O - OTf]$^+$) is seen over 4 days, along with the appearance of a singly-oxygenated sulfoxide species **3** at *m/z* 664.4 ([Fe(LN_3SOMe)(OTf)]$^+$). Further analysis (vide infra) reveals that this complex is likely an Fe^{III} species which was reduced and observed as a monocation in the LDI-MS experiment.

Complex **2** also exhibits reactivity toward O_2. Solutions of compound **2** react with excess O_2 at 60 °C in a closed reaction vessel to afford the sulfone **4** in 96 h (Scheme 4). Fig. 8 shows the loss of **2**(*m/z* 534.4, [**2** – Cl]$^+$) with the concurrent appearance of a peak at *m/z* 566.4, corresponding to the doubly-oxygenated species [Fe($LN_3S(O_2)$Me)Cl]$^+$. As in the case of **3**, this complex is assigned as an Fe^{III} product but is presumed to be reduced in the LDI-MS experiment to the corresponding monocation. Spectra taken at early time points (0 - 48 h) reveal the presence of a singly oxygenated (possibly sulfoxide) intermediate (*m/z* 550.4, [Fe(LN_3S(O)Me)Cl]$^+$) along with sulfide starting material and sulfone product. This intermediate species is not observed in significant quantities, and after 96 h only the doubly-oxygenated sulfone product **4** was observed (Fig. 10). Attempts to improve the yield of the putative singly-oxygenated complex (*m/z* 550.4) by performing the reaction at lower temperature and pressure gave only small amounts of this species and the doubly-oxygenated product. No significant improvement in yield could be obtained.

Control experiments were conducted, and exposure of 2-aminothiophenol to excess O_2 under the same conditions for 3 d resulted in no observed sulfoxide or sulfone products as measured by ^{1}H-NMR. These control reactions indicated that the presence of the ferrous complexes **1** and **2** were necessary for the observed reactivity.

2.4.2 ^{18}O-labeled water—The reaction of **1** was run in the presence of excess $H_2{}^{18}O$ (100 equiv). This experiment was performed to confirm that dioxygen, and not exogenous water, was the source of the oxygen atom in the sulfoxide complex, and to determine if O-atom exchange with water could occur during the *S*-oxygenation reaction. High-valent ferryl

(Fe=O) species are known to rapidly exchange with H_2O in nonheme iron complexes, resulting in the incorporation of oxygen derived from water in oxidized substrates [73-75]. No ^{18}O incorporation into **3** was observed by LDI-MS in the presence of $^{18}OH_2$. This result indicates that O_2 is the sole source of oxygen in the *S*-oxygenation reaction, and suggests that ferryl intermediates do not play a significant role. In addition, water (in small amounts) does not appear to have any inhibitory effect on this reaction.

2.5. Product characterization

2.5.1. Determination of the iron oxidation state—In our previous S-oxygenation studies, the final product(s) were shown to be in the iron +2 oxidation state, making these complexes good functional models for CDO, and opening up the possibility for catalytic activity. Product complexes **3** and **4** exhibit featureless absorption spectra (Figs. S3 – S4), and also give paramagnetic ^{1}H-NMR spectra (Figs. S5 – S6) with no discernable resonances that can be assigned to ligand-based peaks. ^{1}H-NMR spectra of **3** and **4** are significantly different from the sharp, paramagnetically shifted spectra that is characteristic of high-spin iron(II), as seen in the starting materials **1** and **2** (Figs. S1 – S2). These featureless H-NMR spectra are consistent with high-spin ($S = 5/2$) iron(III)-containing complexes. The X-band EPR spectrum of **3** (Fig. S7) reveals an intense signal near $g_{eff} = 4.28$ that is typical for a rhombic, hs-Fe^{III} ion. There is also a strong feature at $g_{eff} = 2$ that may arise from hs-Fe^{III}, ls-Fe^{III} or intermolecular interactions [76-80]. The EPR spectrum for **4** (Fig. S8) exhibits similar peaks near $g_{eff} = 4.29$ and 2.01, and while detailed simulations of these spectra have not been attempted, they are clearly consistent with the S-oxygenated products **3** complexes **1** and **2**, which are overlayed with the spectra from **3** and **4**, show only very weak signals in the same regions, which can be attributed to a small amount of oxidation by air during sample preparation.

A UV-Vis titration for iron(II) was employed to confirm the oxidation state of the Fe product in these sulfide oxygenation reactions. It is well known that 1,10-phenanthroline is a strong chelator for iron(II) and iron(III), forming highly colored $[Fe(phen)_3]^{2+}$ and $[Fe(phen)_3]^{3+}$ complexes, which exhibit distinct spectra (Fig. S9). Titration of the iron from the crude reaction mixture of **4** with 5.0 equiv of 1,10-phenanthroline (Fig. S10) and comparison of the absorbance at $\lambda = 510$ nm (the marker band for $[Fe(phen)_3]^{2+}$ with a calibration curve (Fig. S11), revealed that there is < 6% Fe^{II} in this solution. These data confirm that **4** contains a ferric (Fe^{III}) center.

2.5.2. Identification of S-oxygenated products—Attempts to crystallize the sulfoxide and sulfone products in Schemes 3 and 4 were unsuccessful. However, the S-oxygenated products were easily identified when the ligand was separated from the metal center and hydrolyzed with aqueous acid into its component organic fragments (Scheme 5). The relevant organic compounds are distinguishable by the respective ^{1}H-NMR chemical shifts of the RSCH3 moiety. The chemical shift for the methyl sulfide of the starting material, 2-(methylthio)aniline, is $\delta(CDCl_3) = 2.34$ (s, 3H), while the corresponding sulfoxide (2-(methylsulfinyl)aniline) and sulfone (2-(methylsulfonyl)aniline) products have chemical shifts $\delta(CDCl_3) = 2.93$ (s, 3H) and 3.03 (s, 3H) [81], respectively. Demetalation of the crude reaction mixture of **3** was accomplished by stirring with 1 M HCl, neutralization with $NaHCO_3$, and separation of the organic layer. Due to the polar nature of the sulfoxide moiety, 2-(methylsulfinyl)aniline was easily separated from other organic material via column chromatography on silica (EtOAc/hexanes) and its structure confirmed by ^{1}H-NMR (Fig. 9), $\delta(CDCl_3) = 2.93$ (s, 3H). Final recovery of 2-(methylsulfinyl)aniline was low (≤ 10%), contrasting the apparent good conversion observed in the LDI-MS (vide infra).

The demetalation of the reaction mixture of **4** was performed as above, but in this case the S-oxygenated fragment, 2-(methylsulfonyl)aniline, co-eluted with other organics and therefore its purification by chromatography was not successful. However, in the crude ^{1}H-NMR spectrum (Fig. 10) following demetalation, we can clearly identify the characteristic resonance of the sulfone (δ ($CDCl_3$) = 3.05), with only minor contributions from the starting sulfide or sulfoxide methyl groups.

Given the above results, ^{1}H-NMR experiments were conducted in an effort to quantitate the crude products immediately following aqueous workup but prior to chromatographic separation (Figs. S12 – S13). The addition of CH_3NO_2 as an external standard (δ($CDCl_3$) = 4.32) and comparison with the S-oxygenated products (2-(methylsulfinyl)aniline or 2-(methylsulfonyl)aniline, (δ($CDCl_3$) = 2.92 or 3.05, respectively) gives only modest yields of sulfoxide (15%) and sulfone (29%). However, low recovery of other organic ligand fragments was also observed when compared with the CH_3NO_2 standard, indicating that the polar, amino-functionalized fragments are likely lost in the aqueous workup. A comparison of the methyl resonances from the sulfoxide and sulfone with the recovered 2,6-diisopropylaniline resonance (δ($CDCl_3$) = 1.27, d 12H) as an internal standard indicate a higher overall yield of the sulfoxide (51%) and sulfone (45%) products.

3. conclusions

Herein we have reported the synthesis of two unsymmetrical sulfide-incorporated, bis(imino)pyridine complexes which are accessible via a metal-assisted template reaction. Complexes **1** and **2** were characterized by single crystal X-ray crystallography. These complexes react with O_2 at modestly elevated temperature to yield S-oxygenated sulfoxide or sulfone complexes. The identities of the products were determined by mass spectrometry and ^{1}H-NMR studies. UV-Vis quantitation of the iron(II) ions with 1,10-phenanthroline in the reaction mixture of **4** indicated that **4** should contain mainly iron(III) ions. EPR spectroscopy of reaction mixtures following oxygenation confirmed the presence of hs-Fe^{III} complexes in the case of both **3** and **4**. Sulfide oxidation was confirmed by demetalation and hydrolysis of the bis(imino)pyridine ligands in **3** and **4**. The ^{1}H-NMR of the ligand fragments allowed for identification of the sulfoxide and sulfone products from complexes **3** and **4**, respectively. The S-oxygenation reaction for sulfide ligands with dioxygen as the oxidant/O-atom source was demonstrated for two nonheme iron(II) complexes. The nature of the complexes (chloride versus triflate starting materials) determines the extent of S-oxygenation, resulting in either sulfoxide or sulfone products. Selective oxidation of organic substrates such as sulfides is an important and desirable property of metal-mediated oxygenations, and the reactivity reported here warrants further investigation.

4. Experimental

4.1. General Remarks

All reagents were purchased from commercial vendors and used without further purification unless noted otherwise. All reactions were carried out under an atmosphere of N_2 inside a glovebox or under Ar by standard Schlenk and vacuum line techniques unless otherwise noted. Dioxygen gas (2.6 Grade) was purchased from BOC Gases and dried by passage through a column of Drierite. $H_2{}^{18}O$ (97%) was purchased from Cambridge Isotope Laboratories, Inc. Iron(II) trifluoromethanesulfonate (98%) was purchased from Strem. Iron(II) chloride (98%), 2-(methylthio)aniline (97%), and 2,6-diacetylpyridine (99%) were purchased from Sigma-Aldrich. 2,6-diisopropylaniline (92%) was purchased from Acros. Dichloromethane was purified via a Pure-Solv Solvent Purification System from Innovative Technology, Inc. Methanol, ethanol, and triethylamine were distilled over CaH_2. All solvents were degassed by repeated cycles of freeze-pump-thaw and stored in an N_2-filled

glovebox. 2-(O=CMe)-6-(2,6-($^{i}Pr_2$-C_6H_3N=CMe)-C_5H_3N was synthesized according to the published procedure (C. Bianchini, G. Mantovani, A. Meli, F. Migliacci, F. Zanobini, F. Laschi, A. Sommazzi, Eur. J. Inorg. Chem. (2003) 1620). LDI-TOF mass spectra were obtained using a Bruker Autoflex III Maldi ToF/ToF instrument (Billerica, MA). Samples were dissolved in CH_2Cl_2 and deposited on the target plate. Samples were irradiated with a 355 nm UV laser and mass analyzed by ToF mass spectrometry in the reflectron/linear mode. High resolution EI mass spectra were obtained using a VG70S double-focusing magnetic sector mass spectrometer (VG Analytical, Manchester, UK, now Micromass/Waters) equipped with an MSS data acquisition system (MasCom, Bremen, Germany). Attenuated total reflectance (ATR) infrared spectra of neat crystalline material and crude reaction mixtures were obtained with a Golden Gate Reflectance diamond cell in a Nexus 670 Thermo-Nicolet FTIR spectrometer. Crude reaction mixtures were deposited on the reflectance window as a solution in CH_2Cl_2 and allowed to dry to a residue. Electron paramagnetic resonance (EPR) spectra were obtained on a Bruker Elexsys E580 EPR spectrometer with a Bruker super high Q resonator (SHQE) at 15 K. The EPR spectrometer was equipped with an Oxford Instruments ESR900 liquid helium flow cryostat.

4.2. Synthesis

4.2.1. Synthesis of [$Fe^{II}(LN_3SMe)(H_2O)_3](OTf)_2$•$Et_3NHOTf$, 1•$Et_3NHOTf$—An amount of 2-(O=CMe)-6-(2,6-($^{i}Pr_2$-C_6H_3N=CMe)-C_5H_3N (200 mg, 0.62 mmol) and $Fe(OTf)_2$ (230 mg, 0.65 mmol) were suspended in EtOH (10 mL) and heated at 60 °C for 1 h. The solids slowly dissolved to give a deep purple solution, and a solution of 2-(methylthio)aniline (73 μL, 0.62 mmol) and triethylamine (22 μL, 0.62 mmol) in EtOH (1 mL) was added to the reaction mixture. The reaction was stirred at 80 °C for 24 h to give a dark red solution that was then cooled to room temperature. The crude reaction mixture was evaporated to dryness and the resulting solid residue was brought into a glovebox, where it was dissolved in a minimum amount of CH_2Cl_2 and filtered through Celite. The filtrate was layered with pentane to give 650 mg (95% yield) of **1** as a dark red residue. Single crystals (red-purple blocks) suitable for X-ray diffraction were grown from slow vapor diffusion of diisopropyl ether into a solution of **1** in MeCN. LDIMS (+): *m/z* 648.3 [**1**-$3H_2O$-OTf]$^{+}$. ATR-IR, ν (cm^{-1}): 3275, 2974, 1589, 1468, 1371, 1291, 1210, 1166, 1098, 1024, 803, 766, 636. *Anal. Calc.* for [$Fe^{II}(L_3NSMe)(H_2O)_3](OTf)_2$ • 0.5 $Et_3NH^{+}OTf^{-}{}_3(C_{33.5}H_{47}F_{7.5}FeN_{3.5}O_{10.5}S_{3.5})$: Predicted: C, 41.17; H, 4.85; N, 5.02. Found: C, 41.29; H 5.02; N, 5.24. Note: Although the X-ray structure of **1** contains one $EtNH^{+}$ OTf per Fe, samples for elemental analysis contain crystalline material along with inseparable residue. Elemental data for the bulk material fits best for 0.5 Et_3NH^{+} OTf^{-} per *Fe*.

4.2.2 Synthesis of [Fe^{II} ($LN_3SMe)Cl_2$]· MeOH, 2• MeOH—An amount of 2-(O=CMe)-6-(2,6-(^{i}Pr2-C_6H_3N=CMe)-C_5 H_3N (200 mg, 0.62 mmol) and $FeCl_2$ (230 mg, 0.65 mmol) were suspended in EtOH (10 mL) and heated at 60 °C for 1 h. The solids slowly dissolved to give a deep blue solution, and a solution of 2-(methylthio)aniline (73 μL, 0.62 mmol) and triethylamine (22 μL, 0.62 mmol) in EtOH (1 mL) was added to the reaction mixture. The reaction was stirred at 80 °C for 24 h and then cooled to room temperature. The crude reaction mixture was evaporated to dryness and the resulting solid residue was brought into a glovebox where it was dissolved in a minimum amount of CH_2Cl_2 and filtered through Celite. Layering the filtrate with pentane gave 250 mg (72% yield) of **2** as a dark blue residue. Single crystals of **2**•MeOH for X-ray diffraction were prepared by slow vapor diffusion of diisopropyl ether into a MeOH solution of **2**. LDIMS (+): *m/z* 534.3 [**2**-Cl]$^{+}$. ATR-IR, ν (cm^{-1}): 2964, 1585, 1463, 1370, 1318, 1269, 1204, 1105, 1059, 939, 803, 778, 738. *Anal. Calc.* for [Fe^{II} ($L_3NSMe)Cl_2$]•MeOH ($C_{29}H_{37}Cl_2FeN_3OS$): Predicted: C, 57.82; H, 6.19; N, 6.97. Found: C, 57.74; H 6.30; N, 7.03.

4.3. O_2 Reactivity

4.3.1. Oxidation of l with O_2—Compound **1**•0.5 $Et_3NH^+OTf^-$ (50.0 mg, 51 μmol) was dissolved in 5 mL of CH_2Cl_2 and transferred to a pressure vessel equipped with a vacuum port. Excess O_2(g) was bubbled into the solution for 5 min and the vessel was put under an atmosphere of O_2 before being sealed and heated to 60 °C. The reaction was monitored by removal of aliquots of the reaction mixture for analysis by LDI-MS. Complete disappearance of the starting material was observed after 96 h. The crude reaction mixture was then stirred with 5 mL of 1 M HCl for 1 h before being neutralized with $NaHCO_3$. The organic layer was then collected, dried, and 2-(methylsulfinyl)aniline was purified by column chromatography on silica with EtOAc/hexanes. ^{1}H-NMR ($CDCl_3$) (@ 25 °C) δ 7.23-7.22 (m, 2H), 6.75 (t, 1H), 6.69 (d, 1H), 2.93 (s, 3H). This spectrum matched that of an authentic sample prepared as described in section *4.3.5*.

4.3.2. $H_2{}^{18}O$ study—Compound **1**•0.5 $Et_3NH^+OTf^-$ (34 mg, 35 μmol) was dissolved in 3.0 mL of CH_2Cl_2 and $H_2{}^{18}$ O (60 μL, 100 equiv) was added. The mixture was transferred to a reaction vessel and $^{16}O_2$(g) was bubbled through the solution or 5 min. The vessel was sealed and heated to 60 °C for 96 h. The LDI-MS of the crude reaction mixture showed an isotopic cluster at *m/z* 684.1 for the unlabeled sulfoxide **3**, and no significant peak corresponding to ^{18}O incorporation at *m/z* 686.1 was observed.

4.3.4. Oxidation of 2 with O_2—Compound **2**•MeOH (14.0 mg, 23 μmol) was dissolved in 5.0 mL of CH_2Cl_2 and transferred to a pressure vessel equipped with a side-arm. Excess O_2(g) was bubbled into the solution for 5 min and the vessel was put under a slight positive pressure of O_2 before being sealed and heated to 60 °C. The reaction was monitored by LDI-MS over the course of several days. After 96 h the reaction was complete as evidenced by the absence of peaks for either the sulfide starting material or sulfoxide intermediate observed in the LDI-MS spectrum. The crude reaction mixture was then stirred with 5 mL of 1 M HCl for 1 h before being neutralized with $NaHCO_3$. The organic layer was then collected and dried. The ^{1}H-NMR spectrum of the crude mixture allowed for the identification of the S-oxygenated product, 2-(methylsulfonyl)aniline, δ ($CDCl_3$) = 3.06. This peak corresponds to the literature value [81].

4.3.5. Synthesis of 2-(methylsulfinyl)aniline—An amount of 2-(methylthio)aniline (44 mg, 0.316 mmol) was dissolved in 7 mL of CH_2Cl_2 and *m*CPBA (55 mg, 0.316 mmol) was added dropwise as a solution in 3 mL of CH_2Cl_2. After stirring for several minutes, TLC analysis indicated the reaction was complete, and the product was purified by column chromatography on silica (EtOAc/hexanes) to give 10 mg (20 % yield) of a pale solid. ^{1}H-NMR ($CDCl_3$) (@ 25 °C) δ 7.27-7.22 (m, 2H), 6.75 (t, 1H), 6.69 (d, 1H), 2.93 (s, 3H). MS (EI+) *m/z* 155.1 [M^+].

Supplementary Material

Refer to Web version on PubMed Central for supplementary material.

Acknowledgments

The NIH (GM62309) is gratefully acknowledged for financial support. We thank Dr. Veronika Szalai and Dr. R. Adam Kinney for assistance with EPR measurements.

References

1. Bollinger JM Jr, Krebs C. J Inorg Biochem. 2006; 100:586. [PubMed: 16513177]

2. Solomon EI, Brunold TC, Davis MI, Kemsley JN, Lee SK, Lehnert N, Neese F, Skulan AJ, Yang YS. J Zhou, Chem Rev. 2000; 100:235.
3. Costas M, Mehn MP, Jensen MP, Que L Jr. Chem Rev. 2004; 104:939. [PubMed: 14871146]
4. Koehntop KD, Emerson JP, Que L Jr. J Biol Inorg Chem. 2005; 10:87. [PubMed: 15739104]
5. Neidig ML, Solomon EI. Chem Commun. 2005:5843.
6. Ryle MJ, Hausinger RP. Curr Opin Chem Biol. 2002; 6:193. [PubMed: 12039004]
7. Kovaleva EG, Lipscomb JD. Nat Chem Biol. 2008; 4:186. [PubMed: 18277980]
8. Pierce BS, Gardner JD, Bailey LJ, Brunold TC, Fox BG. Biochemistry. 2007; 46:8569. [PubMed: 17602574]
9. Joseph CA, Maroney MJ. Chem Commun. 2007:3338.
10. McCoy JG, Bailey LJ, Bitto E, Bingman CA, Aceti DJ, Fox BG, Phillips GN Jr. Proc Natl Acad Sci U S A. 2006; 103:3084. [PubMed: 16492780]
11. Simmons CR, Liu Q, Huang QQ, Hao Q, Begley TP, Karplus PA, Stipanuk MH. J Biol Chem. 2006; 281:18723. [PubMed: 16611640]
12. Ye S, Wu X, Wei L, Tang DM, Sun P, Bartlam M, Rao ZH. J Biol Chem. 2007; 282:3391. [PubMed: 17135237]
13. Crawford JA, Li W, Pierce BS. Biochemistry. 2011; 50:10241. [PubMed: 21992268]
14. Kumar D, Thiel W, de Visser SP. J Am Chem Soc. 2011; 133:3869. [PubMed: 21344861]
15. Tchesnokov EP, Wilbanks SM, Jameson GNL. Biochemistry. 2012; 51:257. [PubMed: 22122511]
16. Imsand EM, Njeri CW, Ellis HR. Arch Biochem Biophys. 2012; 521:10. [PubMed: 22433531]
17. McDonald AR, Bukowski MR, Farquhar ER, Jackson TA, Koehntop KD, Seo MS, De Hont RF, Stubna A, Halfen JA, Munck E, Nam W, Que L Jr. J Am Chem Soc. 2010; 132:17118. [PubMed: 21070030]
18. Saget T, Lemouzy SJ, Cramer N. Angew Chem Int Ed. 2012; 51:2238.
19. Kalatzis V, Cherqui S, Antignac C, Gasnier B. Embo J. 2001; 20:5940. [PubMed: 11689434]
20. Kalatzis V, Antignac C. Nephrol Dial Transplant. 2002; 17:1883. [PubMed: 12401840]
21. Perry TL, Norman MG, Yong VW, Whiting S, Crichton JU, Hansen S, Kish SJ. Ann Neurol. 1985; 18:482. [PubMed: 4073841]
22. Pean AR, Parsons RB, Waring RH, Williams AC, Ramsden DB. J Neurol Sci. 1995; 129:107. [PubMed: 7595598]
23. Parsons RB, Waring RH, Ramsden DB, Williams AC. Neurotoxicology. 1998; 19:599. [PubMed: 9745917]
24. Cremlyn, RJ. An Introduction to Oragnosulfur Chemistry. John Wiley & Sons; 1996.
25. Page, P., editor. Organosulfur Chemistry. Vol. 2. Academic Press; Great Britain: 1998.
26. Fernández I, Khiar N. Chem Rev. 2003; 103:3651. [PubMed: 12964880]
27. Carreño MC. Chem Rev. 1995; 95:1717.
28. Campos-Martin JM, Capel-Sanchez MC, Fierro JLG. Green Chem. 2004; 6:557.
29. Block, E. Reactions of Organosulfur Compounds. New York: Academic Press; 1978.
30. Riley, D.; Stern, M.; Ebner, J. Activation of Dioxygen and Homogeneous Catalytic Oxidation. Plenum Press; New York, NY, USA: 1993. Industrial Perspectives on the Use of Dioxygen-New Technology to Solve Old Problems; p. 31
31. Kagan, HB.; Luukas, TO. Transition Metals for Organic Synthesis. Beller, MB.; Bolm, C., editors. Vol. Chapter 2.15. Wiley-VCH; 1998. p. 479
32. Te M, Fairbridge C, Ring Z. Appl Catal, A. 2001; 219:267.
33. Li C, Jiang ZX, Gao JB, Yang YX, Wang SJ, Tian FP, Sun FX, Sun XP, Ying PL, Han CR. Chem-Eur J. 2004; 10:2277. [PubMed: 15112217]
34. Ricci LC, Comasseto V, Andrade LH, Capelari M, Cass QB, Porto ALM. Enzyme Microb Technol. 2005; 36:937.
35. Lee HB, Ren T. Inorg Chim Acta. 2009; 362:1467.
36. Khavrutskii IV, Maksimov GM, Kholdeeva OA. React Kinet Catal Lett. 1999; 66:325.
37. Clennan EL, Zhou WH, Chan J. J Org Chem. 2002; 67:9368. [PubMed: 12492340]

38. Choudary BM, Reddy CRV, Prakash BV, Kantam ML, Sreedhar B. Chem Commun. 2003:754.
39. Chen L, Yang Y, Jiang DL. J Am Chem Soc. 2010; 132:9138. [PubMed: 20536239]
40. Baciocchi E, Chiappe C, Del Giacco T, Fasciani C, Lanzalunga O, Lapi A, Melai B. Org Lett. 2009; 11:1413. [PubMed: 19228056]
41. Legros J, Bolm C. Angew Chem Int Ed. 2003; 42:5487.
42. Boring E, Geletii YV, Hill CL. J Am Chem Soc. 2001; 123:1625. [PubMed: 11456761]
43. Rao TV, Sain B, Kumar K, Murthy PS, Prasada Rao TSR, Joshi GC. Synth Commun. 1998; 28:319.
44. Wang F, Zhang H, Song GQ, Lu XL. Synth Commun. 1999; 29:11.
45. Song GQ, Wang F, Zhang H, Lu XL, Wang C. Synth Commun. 1998; 28:2783.
46. Bagherzadeh M, Amini M. Inorg Chem Commun. 2009; 12:21.
47. Ji HB, Wang TT, Wang LF, Fang YX. React Kinet Catal Lett. 2007; 90:259.
48. Bosch E, Kochi JK. J Org Chem. 1995; 60:3172.
49. Martín SE, Rossi LI. Tetrahedron Lett. 2001; 42:7147.
50. Gao JB, Lu L, Zhou WJ, Gao GH, He MY. J Porous Mater. 2008; 15:127.
51. Kinen CO, Rossi LI, de Rossi RH. Green Chem. 2009; 11:223.
52. Okun NM, Tarr JC, Hilleshiem DA, Zhang L, Hardcastle KI, Hill CL. J Mol Catal A: Chem. 2006; 246:11.
53. Santoni G, Licini G, Rehder D. Chem-Eur J. 2003; 9:4700. [PubMed: 14566876]
54. Nakajima K, Kojima M, Toriumi K, Saito K, Fujita J. Bull Chem Soc Jpn. 1989; 62:760.
55. Mba M, Pontini M, Lovat S, Zonta C, Bernardinelli G, Kundig PE, Licini G. Inorg Chem. 2008; 47:8616. [PubMed: 18774797]
56. Maurya MR, Khan AA, Azam A, Kumar A, Ranjan S, Mondal N, Pessoa JC. Eur J Inorg Chem. 2009:5377.
57. Lippold I, Becher J, Klemm D, Plass W. J Mol Catal A: Chem. 2009; 299:12.
58. Werncke CG, Limberg C, Knispel C, Metzinger R, Braun B. Chem-Eur J. 2011; 17:2931. [PubMed: 21290437]
59. Guo CY, Wang YY, Xu KZ, Zhu HL, Liu P, Shi QZ, Peng SM. Polyhedron. 2008; 27:3529.
60. Lovat S, Mba M, Abbenhuis HCL, Vogt D, Zonta C, Licini G. Inorg Chem. 2009; 48:4724. [PubMed: 19382778]
61. Kinen CO, Rossi LI, de Rossi RH. J Org Chem. 2009; 74:7132. [PubMed: 19691326]
62. Rossi LI, Martin SE. Appl Catal, A. 2003; 250:271.
63. Luo Z, Geletii YV, Hillesheim DA, Wang YM, Hill CL. ACS Catal. 2011; 1:1364.
64. Jiang YB, Widger LR, Kasper GD, Siegler MA, Goldberg DP. J Am Chem Soc. 2010; 132:12214. [PubMed: 20712312]
65. Badiei YM, Siegler MA, Goldberg DP. J Am Chem Soc. 2011; 133:1274. [PubMed: 21207980]
66. McQuilken AC, Jiang YB, Siegler MA, Goldberg DP. J Am Chem Soc. 2012; 134:8758. [PubMed: 22578255]
67. Sallmann M, Siewert I, Fohlmeister L, Limberg C, Knispel C. Angew Chem Int Ed. 2012; 51:2234.
68. Bianchini C, Mantovani G, Meli A, Migliacci F, Zanobini F, Laschi F, Sommazzi A. Eur J Inorg Chem. 2003:1620.
69. Badiei YM, Jiang YB, Widger LR, Siegler MA, Goldberg DP. Inorg Chim Acta. 2012; 382:19.
70. Britovsek GJP, England J, Spitzmesser SK, White AJP, Williams DJ. Dalton Trans. 2005:945. [PubMed: 15726149]
71. Krishnamurthy D, Sarjeant AN, Goldberg DP, Caneschi A, Totti F, Zakharov LN, Rheingold AL. Chem-Eur J. 2005; 11:7328. [PubMed: 16144021]
72. Small BL, Brookhart M, Bennett AMA. J Am Chem Soc. 1998; 120:4049.
73. Nam W. Acc Chem Res. 2007; 40:522. [PubMed: 17469792]
74. Seo MS, In JH, Kim SO, Oh NY, Hong J, Kim J, Que L Jr, Nam W. Angew Chem Int Ed. 2004; 43:2417.

75. Que L Jr. Acc Chem Res. 2007; 40:493. [PubMed: 17595051]
76. Weisser JT, Nilges MJ, Sever MJ, Wilker JJ. Inorg Chem. 2006; 45:7736. [PubMed: 16961365]
77. Guerra KP, Delgado R. Polyhedron. 2008; 27:2265.
78. Taylor SW, Chase DB, Emptage MH, Nelson MJ, Waite JH. Inorg Chem. 1996; 35:7572.
79. Meyer K, Bill E, Mienert B, Weyhermüller T, Wieghardt K. J Am Chem Soc. 1999; 121:4859.
80. Comba P, Gahan LR, Mereacre V, Hanson GR, Powell AK, Schenk G, Zajaczkowski-Fischer M. Inorg Chem. 2012; 2012:12195.
81. Andersen KK, Chumpradit S, Mcintyre DJ. J Org Chem. 1988; 53:4667.

The unsymmetrical iron(II) bis(imino)pyridine complexes $[Fe^{II}(LN_3SMe)(H_2O)_3](OTf)_2$ (**1**), and $[Fe^{II}(LN_3SMe)Cl_2]$ (**2**) were synthesized and characterized by X-ray crystallography. Complexes **1** and **2** react with molecular oxygen under identical conditions to afford sulfoxide and sulfone products, respectively.

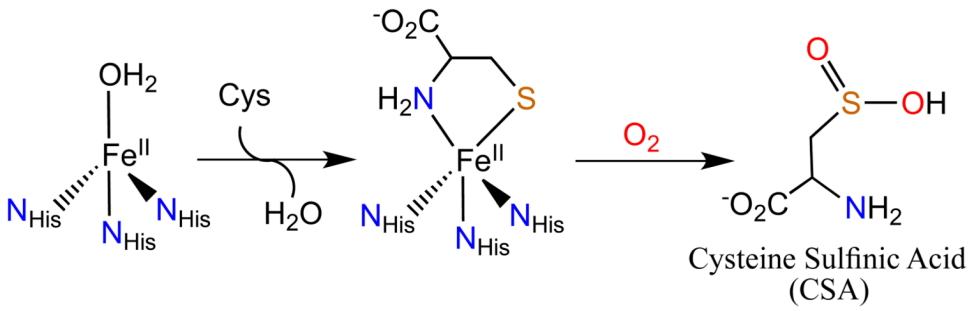

Fig. 1.
Oxidation of cysteine to cysteine sulfinic acid by CDO.

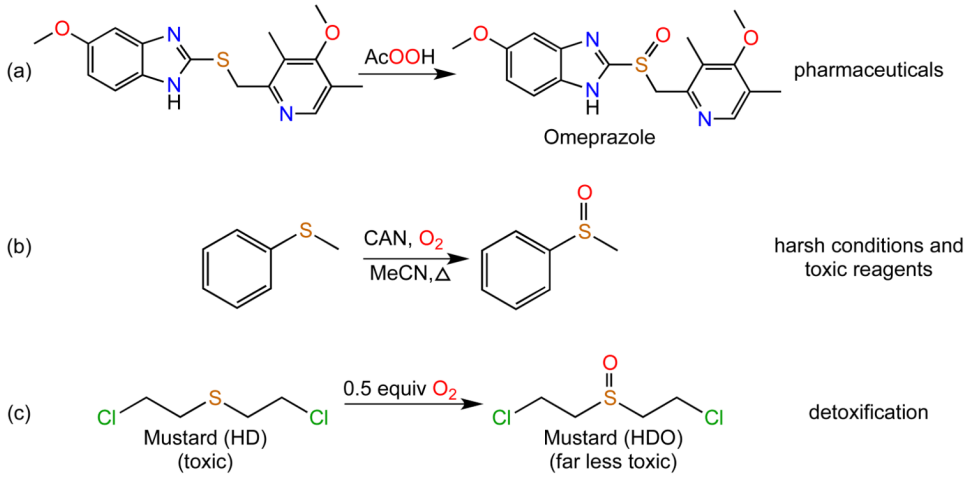

Fig. 2.
Examples of sulfoxides in synthetic chemistry and detoxification processes.

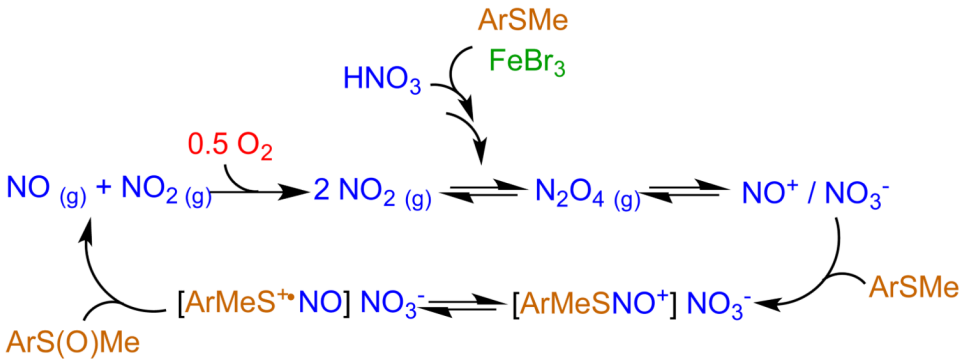

Fig. 3.
Proposed catalytic mechanism of aerobic sulfoxidation by NO_x species [61].

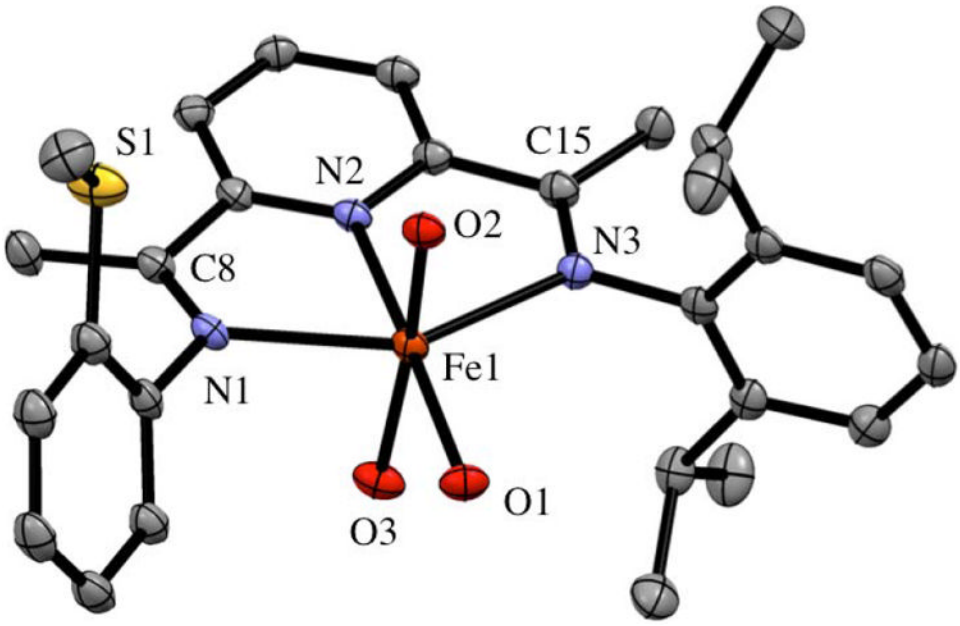

Fig. 4.
Displacement ellipsoid plot (50% probability level) of the cation of **1**. H-atoms are removed for clarity.

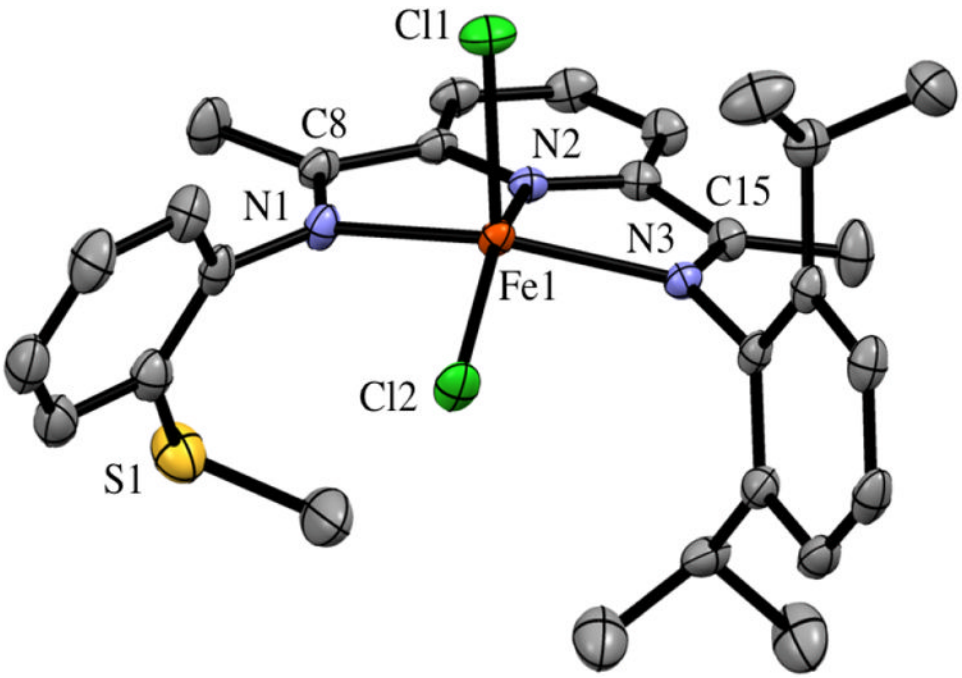

Fig. 5.
Displacement ellipsoid plot (50% probability level) of **2**. H-atoms are removed for clarity.

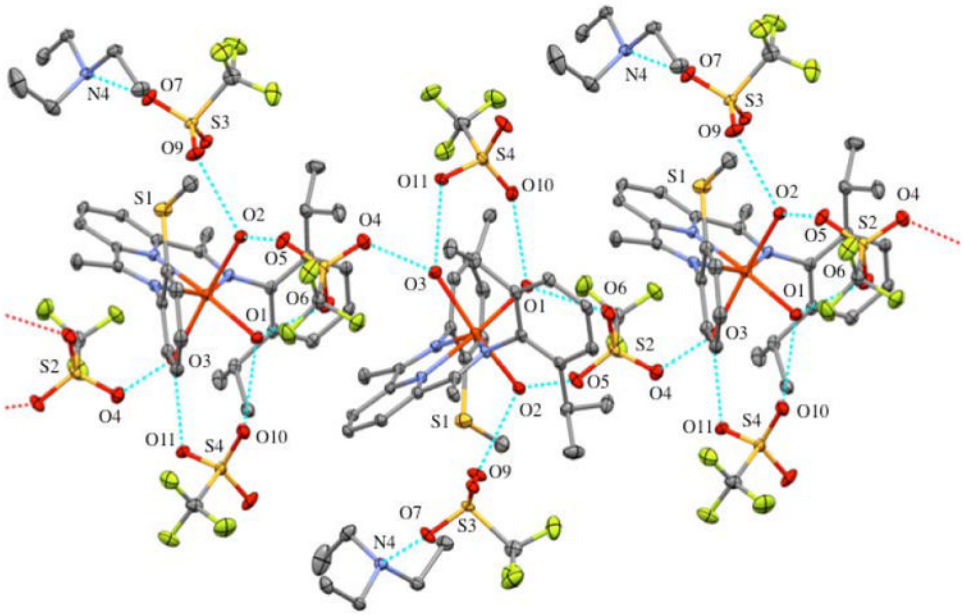

Fig. 6.

Hydrogen bonding network in the crystal lattice of **1**. Disorder and H-atoms were removed for clarity.

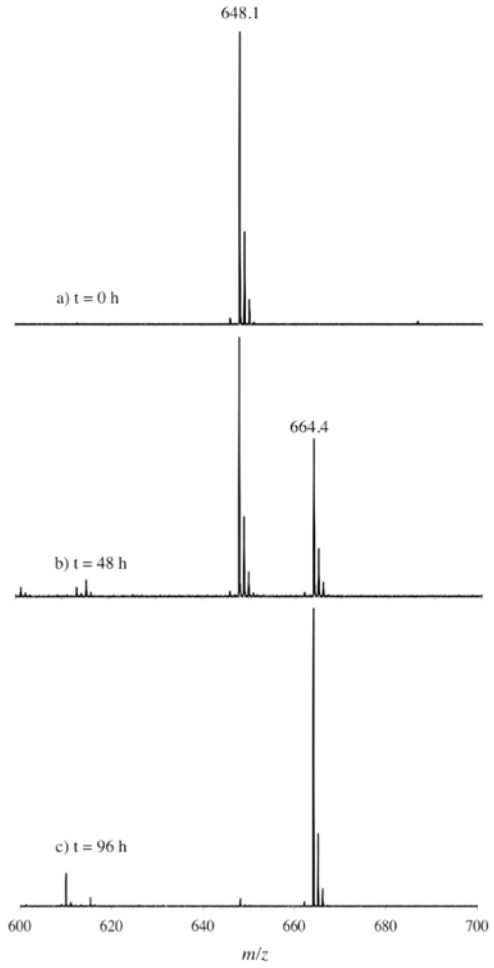

Fig. 7.

Reaction of **1** with excess O_2 in CH_2Cl_2 at 60 °C as monitored by LDI-MS. The peak at *m/z* 648.1 is assigned to $[\mathbf{1} - 3H_2O - OTf]^+$, and the peak at *m/z* 664.4 is assigned to $[Fe(LN_3S(O)Me)(OTf)]^+$.

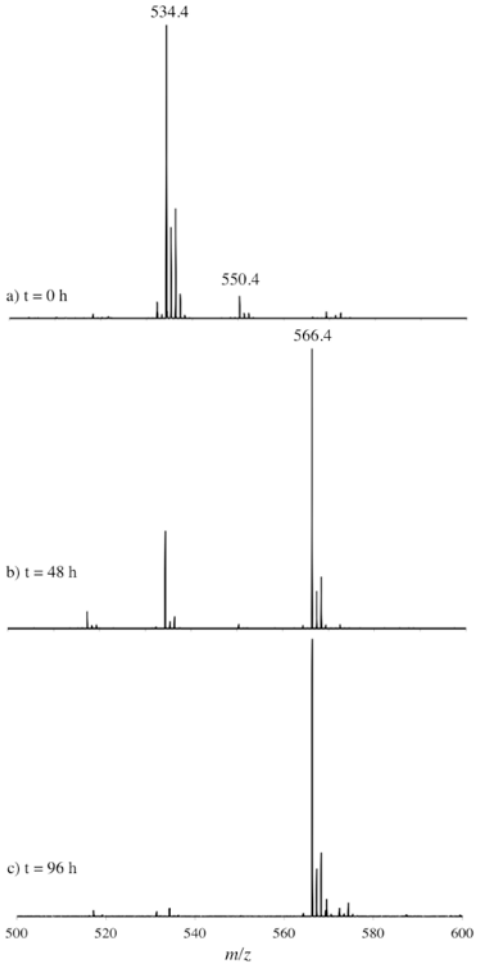

Fig. 8.

Reaction of **2** with excess O_2 in CH_2Cl_2 at 60 °C as monitored by LDI-MS. The peak at *m/z* 534.4 is assigned to $[\mathbf{2} - Cl]^+$, and the peak at *m/z* 566.4 is assigned to doubly-oxygenated $[Fe(LN_3S(O_2)Me)Cl]^+$. The small peak at *m/z* 550.4 is assigned to singly-oxygenated $[Fe(LN_3S(O)Me)Cl]^+$.

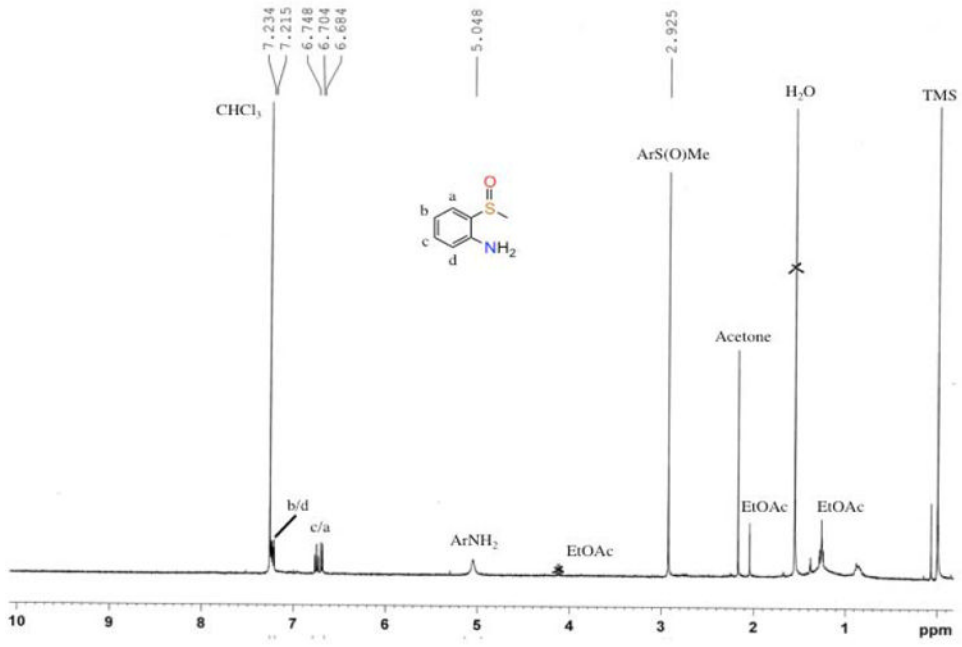

Fig. 9.
^{1}H-NMR spectrum of 2-(methylsulfinyl)aniline recovered following demetalation of **3**.

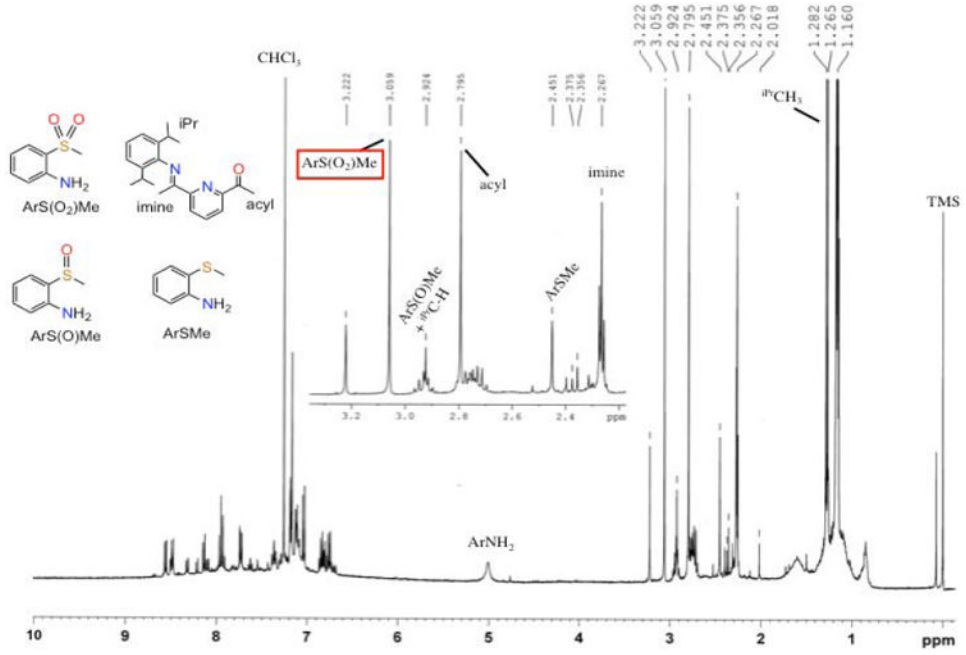

Fig. 10.

^{1}H-NMR spectrum of the crude mixture following demetalation of **4.** The 2-(methylsulfonyl)aniline is identified at 3.06 ppm, with minor peaks arising from the intermediate sulfoxide (2.92 ppm) and starting sulfide (2.36 ppm).

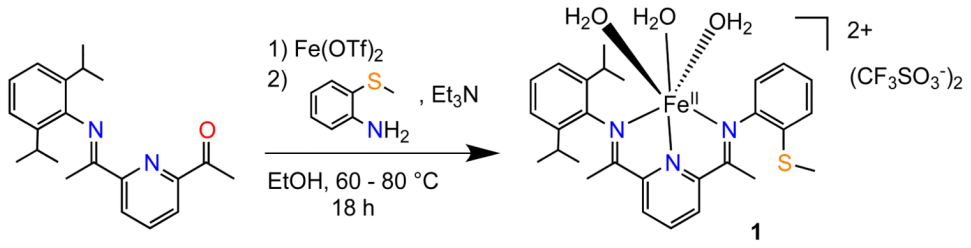

Scheme 1.
Synthesis of complex **1**.

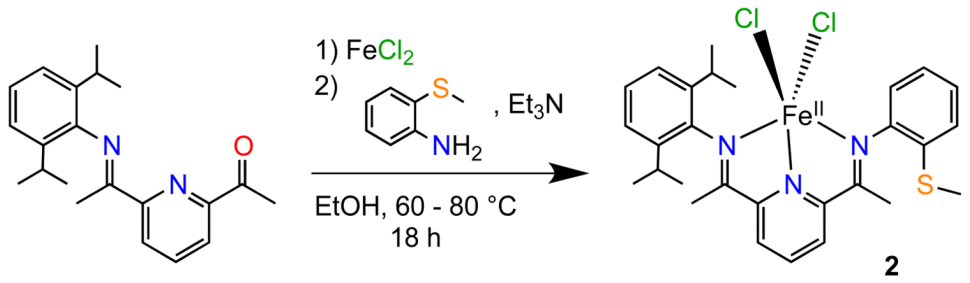

Scheme 2.
Synthesis of complex **2**.

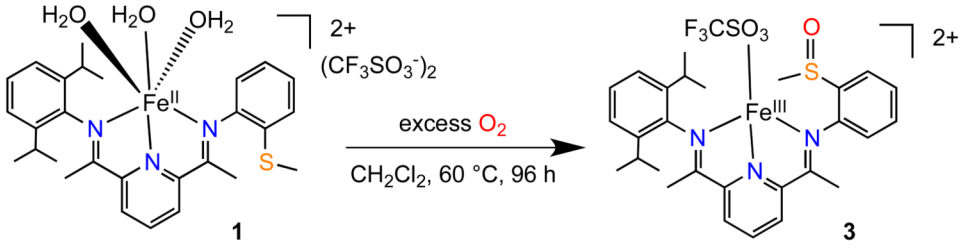

Scheme 3.
Reaction of **1** with O_2 to form sulfoxide complex **3**.

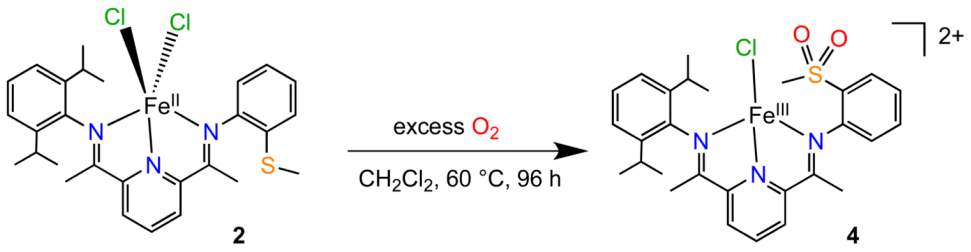

Scheme 4.
Reaction of **2** with O_2 to form the sulfone complex **4**.

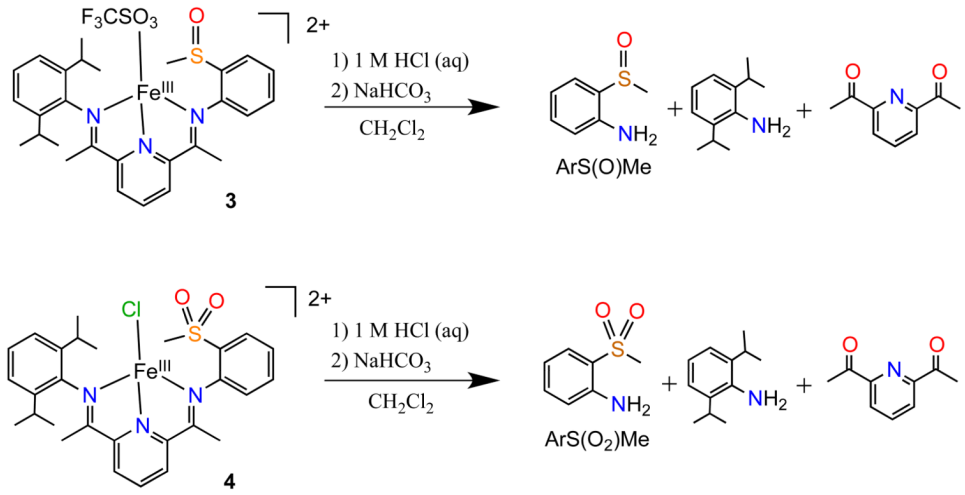

Scheme 5.
Hydrolysis of bis(imino)pyridine complexes.

Table 1

Summary of the crystallographic data.

	1•Et_3NHOTf	**2•MeOH**
Formula	$[C_{37}H_{55}FeN_4O_{12}S_4F_9]$	$[C_{29}H_{37}Cl_2FeN_3OS]$
Formula weight	1102.94	602.43
T (K)	110	110
Color	Red-purple	Dark blue
Class	monoclinic	monoclinic
Space group	$P2_1/n$	$P2_1/c$
a (Å)	13.73725(19)	9.86440(19)
b (Å)	16.1292(2)	16.3351(2)
c (Å)	22.9656(3)	18.2562(2)
β (°)	95.0312(13)	94.1396(15)
V (Å^3)	5068.90(12)	2934.07(7)
Z	4	4
ρ (g cm^{-3})	1.445	1.364
μ (mm^{-1})	0.553	0.794
θ (°)	25	26.25
No. reflections collected	36550	24149
No. unique reflections	8932	5932
R_{int}	0.0459	0.0274
No. variable parameters	821	358
R [$I > 2\ (I)$] 1	0.0450	0.0422
wR [$I > 2\ (I)$] 2	0.1222	0.1078
R_1 [all data]	0.0642	0.0467
wR_2 [all data]	0.1292	0.1103
Goodness-of-fit (GOF) on F^2	1.041	1.084
Largest difference in hole and peak (eA^{-3})	−0.58 and 0.65	−0.83 and 1.03

Table 2

Selected bond distances (Å) and bond angles (°) for iron(II) complexes.

	1	$[Fe^{II}(^{iPr}BIP)(H_2O)_2(NCCH_3)](OTf)_2$[a]	2	$[Fe^{II}(^{iPr}BIP)Cl_2]$[b]
Fe1-N1	2.245(2)	2.276(3)	2.200(2)	2.222(4)
Fe1-N2	2.102(2)	2.086(3)	2.094(2)	2.091(4)
Fe1-N3	2.234(2)	2.280(3)	2.186(2)	2.225(5)
Fe1-O1	2.086(2)	2.075(2)	N/A	N/A
Fe1-O2	2.098(2)	2.161(2)	N/A	N/A
Fe1-O3	2.116(2)	N/A	N/A	N/A
Fe-N4	N/A	2.105(5)	N/A	N/A
Fe-Cl1	N/A	N/A	2.3297(7)	2.3173(19)
Fe-Cl2	N/A	N/A	2.2611(7)	2.2627(17)
N1-C8	1.281(4)	1.286(4)	1.287(4)	1.301(7)
N3-C15	1.287(4)	1.284(4)	1.288(3)	1.295(7)
N1-Fe1-N2	73.30(8)	74.20(10)	73.14(8)	73.67(16)
N1-Fe1-N3	146.95(8)	147.36(9)	141.43(8)	140.23(16)
N2-Fe1-N3	73.89(8)	74.03(10)	73.11(7)	72.59(16)
N2-Fe1-O1	176.45(9)	102.98(10)	N/A	N/A
N2-Fe1-O2	96.69(8)	83.08(9)	N/A	N/A
N2-Fe1-O3	89.82(9)	N/A	N/A	N/A
N2-Fe1-N4	N/A	168.56(10)	N/A	N/A
N2-Fe1-Cl1	N/A	N/A	99.60(6)	94.52(13)
N2-Fe1-Cl2	N/A	N/A	152.16(6)	147.90(13)
O1-Fe1-O2	86.79(8)	173.40(10)	N/A	N/A
Cl1-Fe1-Cl2	N/A	N/A	108.06(3)	117.58(7)
O1-Fe1-N4	86.64(9)	87.59(10)	N/A	N/A
O2-Fe1-N4	170.14(8)	86.58(10)	N/A	N/A

[a] Ref [65].

[b] Ref [72].

Table 3

Selected bond distances (Å) and angles (°) for H-bonding interactions in the solid-state structure of **1**.

Donor Atom (D)	Hydrogen Atom (H)	Acceptor Atom (A)	Distance D-H	Distance H-A	Distance D-A	Bond Angle DHA
O1	H1W1	O6	0.82(2)	1.95(2)	2.759(3)	174(4)
O1	H1W2	O10	0.84(2)	1.99(3)	2.793(3)	160(4)
O1	H1W2	O10′	0.84(2)	1.94(2)	2.77(2)	174(4)
O2	H2W1	O9	0.85(2)	1.90(2)	2.745(6)	171(3)
O2	H2W1	O9′	0.85(2)	1.81(3)	2.636(19)	163(4)
O2	H2W2	O5	0.79(2)	2.01(2)	2.789(3)	171(4)
O3	H3W1	O4	0.82(2)	2.07(3)	2.864(3)	157(3)
O3	H3W2	O11	0.84(2)	1.87(3)	2.702(4)	170(4)
N4	H4A	O7	0.93	1.90	2.755(6)	152